Open Academic Journal of Advanced Science and Technology
ISSN 2577-7807
Vol. 4, No. 2, pp. 30-44.
2020
DOI: 10.33094/5.2017.2020.42.30.44

Cyclic Voltammetry, Kinetics, Thermodynamic and Molecular Docking Parameters for the Interaction of Nickel Chloride with Diphenylthiocarbazone

Esam.A.Gomaa[1*]
Adel.Z. EL-Sonbati[2]
Mostafa.A.Diab[3]
Mohamed.S.EL-Ghareib[4]
Hanaa.M.Salama[5]

[1]*Chemistry Department, Faculty of Science, Mansoura University, Mansoura, Egypt.*
Email: eahgomaa65@yahoo.com
[2,3]*Chemistry Department, Faculty of Science, Damietta University, Damietta, Egypt.*
[4,5]*Chemistry Department, Faculty of Science, Port Said University, Port Said, Egypt.*
[4]*Email: hana_negm20010@yahoo.com*

Keywords:
Cyclic Voltammograms
NiCl2
Potassium ferrioxalate
Diphenylthiocarbazone
Thermodynamic parameters
Kinetic parameters.

Received: *8 July 2020*
Revised: *13 August 2020*
Accepted: *25 August 2020*
Published: *8 September 2020*
(Corresponding Author)*

Abstract

The electrochemical behavior of nickel chloride in citric acid aqueous solution (0.1M) in the presence of potassium ferrioxalate $K_3Fe(Oxalate)_3$ (KFOx) as moderator sensor and by the use of gold working electrode (GWE) was studied. Since nickel ions do not show any peaks in acidic media, but after adding potassium ferrioxalate $K_3Fe(Oxalate)_3$ (KFOx) as a sensor, two redox peaks of nickel ions were obtained. (KFOx) sensor indicating the appearance of nickel ion peaks. Two redox couples of waves were obtained attributed to [Ni(II)-Ox-Fe(III)]/[Ni(III)-Ox-Fe(III)]and[Ni(II)-Ox-Fe(III)] /[Ni(II)-Ox-Fe(II)]. The cyclic voltammetry for $NiCl_2$ and its interaction with diphenylthiocarbazone, dithizone was studies at three different temperatures, 293.15, 303.15 and 313.15K. Different thermodynamic and kinetic parameters of interaction of nickel ions with dithizone were evaluated from the cyclic voltammograms. The estimated cyclic voltammetry values were discussed. Molecular docking was carried out to predict the binding between diphenylthiocabazone, dithizone ligand with the receptor of human liver cancer (3cmf). We can propose that interaction between the 3cmf receptors and the ligand is possible.

Funding: This study received no specific financial support.
Competing Interests: The authors declare that they have no competing interests.
Acknowledgement: Authors acknowledge staff of Port Said University in Egypt to encourage the student.

1. Introduction

Electron transfer processes are at the center of the reactivity of inorganic complexes [1]. Cyclic voltammetry used in determination mechanism of reactions, a number of electrons transferred through oxidation or reduction process, formal potential, the stoichiometry of a system, heterogeneous rate constants and diffusion coefficient of electroactive species [2].

Cyclic voltammetry is a simple, rapid, high sensitive technique, gives qualitative information about an electrochemical process [3]. It is carried out by measuring the resulting current as a function of the applied potential and powerful method for characterizing the electrochemical behavior of analytics that can be electrochemically oxidized or reduced [4].

Here, we have carried out studies on the redox chemistry of nickel(II) complexes of dithizone ligand in the presence of potassium ferrioxalate $K_3Fe(Oxalate)_3$ (KFOx) using gold electrode.

Gold electrodes behave similarly to platinum, but have limited usefulness in the positive potential range due to the oxidation of its surface. It has been very useful, however, for the preparation of modified electrodes containing surface structures known as self-assembled monolayers (SAMs).

Such complexes have an important role in bioinorganic chemistry and redox enzyme systems [5, 6]. The study of structural and binding features of nickel metal complexes can play an important role in better understanding of the biological process [7]. Redox properties of a drug can give insight into its metabolic or pharmaceutical activity [7].

Cyclic voltammetry for nickel salts is necessary as fast technique and gives analytical data about the electrochemical redox reactions for nickel salts with active organic ligands in aqueous media. The complexation ability can be followed from the change in both peak heights and wave potentials for the selected cyclic voltammograms. The shift in half wave potentials can also be applied for studying the complex behaviors in different solution phases. Other authors use different techniques for studying the complexation results from interaction between metal ion and organic ligands, like conductivity, potentiometry, polarography, UV and visible spectroscopy [8].

2. Experimental

Docking Server [9] Gasteiger partial charges were added to the ligand atoms. Non-polar hydrogen atoms were merged, and rotatable bonds were defined. Docking calculations were carried out on dithizone protein model. Essential hydrogen atoms, Kollman united atom type charges, and solvation parameters were added with the aid of AutoDock tools [10]. Affinity grid points and 0.375 Å spacing were generated using the Autogrid program [11]. Auto Dock parameter set- and distance-dependent dielectric functions were used in the calculation of the van der Waals and the electrostatic terms, respectively. Docking simulations were performed using the Lamarckian genetic algorithm (LGA) and the Solis & Wets local search method [12]. Initial position, orientation, and torsions of the ligand molecules were set randomly. All rotatable torsions were released during docking. Each docking experiment was derived from 10 different runs that were set to terminate after a maximum of 250000 energy evaluations. The population size was set to 150. During the search, a translational step of 0.2 Å, and quaternion and torsion steps of 5 were applied.

3. Results and Discussion

In the absence of potassium ferrioxalate nickel ions does not show any peak at the used potential region. In presence of potassium ferrioxalate two redox couples at different potentials were obtained due to the formation of two types of nickel –oxaloferrate (Ni-Ox-Fe) as explained in literature on the use of potassium ferricyanide [11, 12].

The two redox couples are attributed to [Ni(II)-Ox-Fe(III)]/[Ni(III)-Ox-Fe(III)] and [Ni(II)-Ox-Fe(III)]/[Ni(II)-Ox-Fe(II)]. The possible electrode reaction mechanisms for the double couple as explained before in case of using potassium ferricyanide are:

$$Ni(III)\text{-}Ox\text{-}Fe(III) + K^+ + e^- \rightleftharpoons K[Ni(II)\text{-}Ox\text{-}Fe(III)] \quad (1)$$

$$K[Ni(II)\text{-}Ox\text{-}Fe(III)] + K^+ + e^- \rightleftharpoons K_2[Ni(II)\text{-}Ox\text{-}Fe(II)] \quad (2)$$

Where the nickel in the coordinated form in Equation1 is first reduced and is followed be the decrease of ferric ion valence in Equation 2 to ferrous ion.

The redox reaction of $NiCl_2$ using gold working electrode (GWE) was studied at equilibrium in presence of isolating and supporting media of citric acid (0.1M) concentration at different temperatures (293.15, 303.15, and 313.15 K).

The obtained cyclic voltammograms were analyzed [11-16] by:

$$i_p=(2.69X10^{-5})n^{3/2}AD^{1/2}\mu^{1/2}C \quad (3)$$

We can use Equation 3, which is known as Randles Sevcik equation to evaluate the diffusion coefficients for the anodic and catholic peaks.

where i_p is the measured current in Ampere, A is the surface electrode area, D is the diffusion coefficient in cm^3/s, μ the scan rate in V/s and C is the Ni ions concentration.

The voltammograms were carried out by the use of gold working electrode (GWE) from starting potential of 1.5V to -1.5V at 293.15K, 1.0V to -1.0V at 303.15K and 0.8V to -0.8V at 313.15 K.

The Ni waves were appeared here in presence of potassium ferrioxalate; otherwise the Ni waves cannot be detected.

The measured cyclic voltammograms depend on $NiCl_2$ movement and transfer of electrons.

$$k_f = k^o\exp(-\alpha nF/RT)(E-E^o) \quad (4)$$

k_f in Equation 4 is the forward electron rate constant; k^o is the standard electron transfer rate constant for the interaction. E is reduction value for the potential and α is the transfer coefficient [17]. By reversing the potential, the reduced species at the gold working electrode (GWE) is oxidized back to the beginning point.

The electron transfer rate constant for the reverse reaction K_r (oxidation) controlled by the use of Equation 5:

$$k_r = k^o\exp((1-\alpha)Nf/RT)(E-E^o) \quad (5)$$

Reversible reactions give separation in potentials with value equal 58/n (at 25 °C). This relation can be used for evaluating the number of electrons consumed and liberated in the redox reactions. For lot of many reversible reactions, the reduction will be faster for obtaining the reduced and oxidized species in equilibrium.

The equilibrium between the two ionic species in solutions can be illustrated by Nernst Equation 6:

$$E = E^{o} - \ln([R]/[O]) \quad (6)$$

where [R] and [O] are the reduced and oxidized forms concentration. Where the reaction is fast, reversible reaction to another place. The reaction is reversible if K^{o} is greater than $0.32\mu^{1/2}$ [18, 19], where μ is the scan rate. Reactions where cyclic voltammograms are a part from each other with increasing scan rates are quasi-reversible reactions.

Some reactions occur by bond breaking, indicating an irreversible reaction. For quasi reversible reactions, peak current are not proportional to $\mu^{1/2}$. Some scientists used half wave potentials for reversible indication for reactions Equation 7:

$$E_{p/2} = E_{1/2} \pm (28/n)mv \quad (7)$$

Positive sign is for reduction process.

3.1. Electrochemical Behavior of $NiCl_2$ in Citric Acid (0.1M) in Presence of $K_3Fe(OX)_3$ Potassium Ferrioxalate

The cyclic voltammograms for $NiCl_2$ with different concentration using gold working electrode in 0.1 M citric acid supporting electrolyte was studied and the data listed in Figure 1. At the measured temperature, we observe one new reduction wave for $NiCl_2$ and one oxidation peak differ from the peaks necessary for the gold electrode alone in 0.1M citric acid.

The reduction mechanism for nickel salt was suggested to proceed as follows:

$$Ni^{2+} + 2e^{-} = Ni \quad (8)$$

The consuming of two electron mechanism in Equation 8 passed through one step at the approximately 1.5V at 293.15K.

The oxidation peaks at approximately -0.5V explaining the reverse direction of Equation 6 indicating its opposite reaction.

The electrochemical kinetic parameters and the scan rates like solution electron transfer rate constant K_s, anodic & cathodic surface coverage (r_a, r_c), cathodic and anodic quantity of electricity (Q_c, Q_a) and αn_a are represented in Table 1 indicating the increase in all the parameters cited by the decrease of different scan rates. Figure 1 gave an indication that the electrochemical processes discussed for $NiCl_2$ in 0.1M citric acid is reversible.

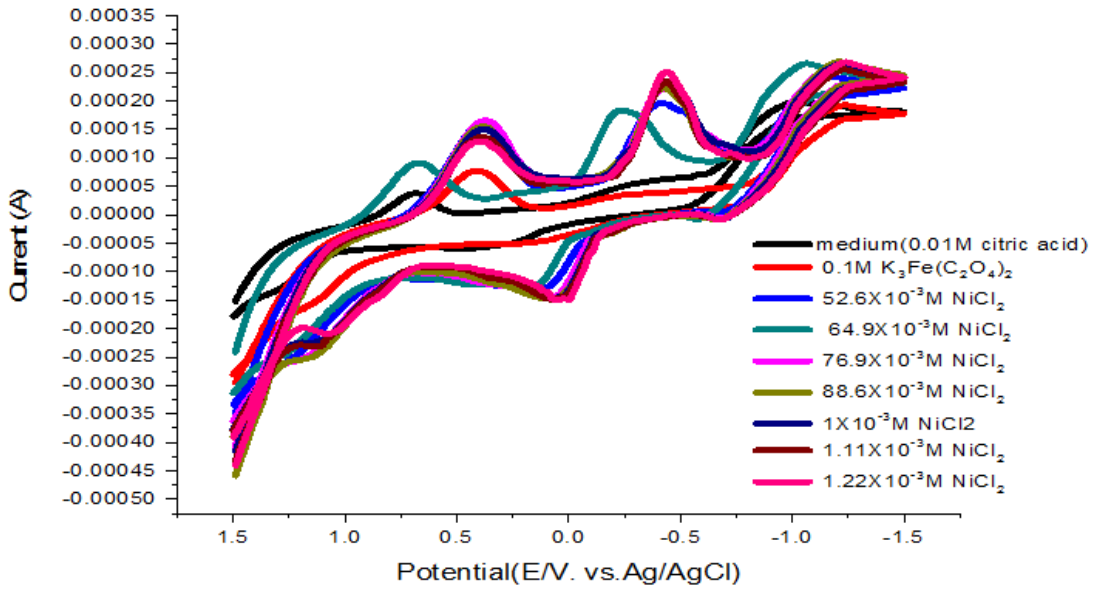

Figure-1. Cyclic voltamogram of $NiCl_2$ (0.1M) in citric acid media at 293.15K.

3.2. Electrochemical behavior of $NiCl_2$ in presence of dithizone (diphenylthiocarbazone) as complexing agent

The cyclic voltammogrames of $NiCl_2$ at different concentrations of dithizone as ligand from the range of $2.38X10^{-4}$ to $8.89X10^{-4}$ M. are shown in Figure 2 . By increasing the concentration of dithizone, there is a shift in $NiCl_2$ reduction peak to more negative potentials. Also positive shift in the oxidation peak was observed. The stability constant (B) and complexion Gibbs free energies are evaluated by the Equation 9:

$$\Delta G = -2{:}303\ RT \log \beta_{MX} \quad (9)$$

The results in Table 2 indicate increasing in complexation ability at 293.15K by the increase in dithizone ligand concentration.

Table-1. Electrochemical parameters of $NiCl_2$ in acidic media at 293.15 K.

M $x10^{-3}$	Ep,a (volt	(-)Ep,c (volt	ΔEp (volt)	(-)ipa $x10^{-5}$ (Amp)	ipc $x10^{-5}$ (Amp)	ipa/ ipc	Da $x10^{-4}$	Dc $x10^{-4}$	(-)Epc/2	αna	ks $x10^{3}$	Γc $x10^{-9}$ (mol/cm2)	(+) Qc $x10^{-5}$	Γa $x10^{-9}$ (mol/cm2)	(-)Qa 10^{-5}
52.6	0.1316	0.4117	0.5433	9.20	0.115	0.799	3.4258	5.37	0.2886	0.3813	2.90	7.6798	5.82	6.1362	4.65
64.9	0.163	0.227	0.39	9.61	0.121	0.794	2.45439	3.89	0.1224	0.4483	0.129	8.0703	6.11	6.408	4.85
76.9	0.0669	0.435	0.4974	0.101	0.151	0.664	1.914	4.34	0.3069	0.3662	1.13	0.10096	7.65	6.704	5.08
88.6	0.0462	0.424	0.4702	0.116	0.152	0.7647	1.926	3.29	0.313	0.4227	0.564	0.10129	7.67	7.746	5.87
1.00	0.0319	0.426	0.4579	0.116	0.163	0.7116	1.513	2.99	0.3242	0.4608	0.439	0.10888	8.25	7.748	5.87
1.11	0.0264	0.437	0.4634	0.103	0.156	0.6619	96.32	2.20	0.3287	0.433	0.408	0.10378	7.86	6.8689	5.20
1.22	-0.0024	0.437	0.4346	0.117	0.190	0.6157	1.0351	2.73	0.3249	0.4187	0.253	0.12694	9.61	7.8155	5.92

Table-2. Electrochemical parameters of complex formation at 293.15 K.

[L] x10-4	Ep,a (volt)	(-)Ep,c (volt)	ΔEp (volt)	(-)ipa $x10^{-5}$ (Amp)	Ipc $x10^{-4}$ (Amp)	ipa/ ipc	Da $x10^{-10}$	Dc $x10^{-10}$	(-)Epc/2	αna	ks	Γc $x10^{-8}$ (mol/cm2)	(+) Qc $x10^{-5}$	Γa $x10^{-9}$ (mol/cm2)	(-)Qa 10^{-5}
2.38	0.0207	0.455	0.4757	8.79	1.89	0.4647	58.297	2.70	0.3424	0.4167	0.565	1.2623	9.56	5.8652	4.44
4.65	0.0242	0.513	-0.4888	0.116	1.95	0.5946	1.0085	2.85	0.3755	-0.0528	1.78	1.2974	9.83	7.7145	5.84
6.82	0.0435	0.567	0.6105	9.62	1.78	0.5407	69.776	2.39	0.4038	0.2875	6.37	1.1868	8.99	6.4167	4.86
8.89	0.0436	0.6136	0.6572	7.64	1.50	0.5101	44.009	1.69	0.4323	0.2587	12.8	9.9893	7.57	5.096	3.86

Table-3. Scan rate effect on the kinetic parameters of complex at 293.15 K.

υ	M x10^{-3}	Ep,a (volt)	(-)Ep,c (volt)	ΔEp (volt)	(-)ipa x10^{-5} (Amp)	ipc x10^{-6} (Amp)	ipa/ ipc	Da x10^{-11}	Dc x10^{-12}	(-)Epc/2	αna	ks x10^{5}	Γc x10^{-9} (mol/cm2)	(+) Qc x10^{-5}	Γa x10^{-9} (mol/cm2)	(-)Qa 10^{-5}
0.01	1.22	0.863	0.379	1.24	2.26	4.52	5.0044	3.8578	1.5404	0.3471	1.47	98.1	3.0149	2.28	15.088	11.4
0.02	1.22	0.8918	0.395	1.287	2.94	6.26	4.6965	3.2585	1.4773	0.3687	1.78	3.63	2.0878	1.58	9.8052	7.43
0.05	1.22	0.9286	0.519	1.448	4.09	0.246	1.6636	2.5274	9.1329	0.4509	0.69	214	3.2831	2.49	5.4616	4.14

Table-4. Electrochemical parameters of $NiCl_2$ in acidic media at 303.15 K.

M x10^{-3}	Ep,a (volt)	(-)Ep,c (volt)	ΔEp (volt)	ipa x10^{-6} (Amp)	ipc x10^{-6} (Amp)	ipa/ ipc	Da x10^{-13}	Dc x10^{-14}	Epc/2	αna	ks x10^{-5}	Γc x10^{-10} (mol/cm2)	(+) Qc x10^{-6}	Γa x10^{-10} (mol/cm2)	Qa 10^{-6}
1	0.1901	0.0191	0.2092	4.09	1.96	2.0862	1.8777	4.3142	0.0136	1.484	5.9179	1.3529	1.0248	2.8226	2.1379
1.22	0.1814	0.0089	0.1904	4.97	1.71	2.9156	1.8635	2.1921	0.0175	1.8281	3.2688	1.1762	0.89083	3.4292	-2.5973
1.43	0.1809	0.0208	0.2017	5.55	2.65	2.0922	1.6895	3.8597	0.0081	1.6768	5.1557	1.8282	1.3847	3.8249	2.897

The rate constant for electron transfer k_s are increased by the increase of dithizone ligand concentration indicating the acceleration of the complex formation.

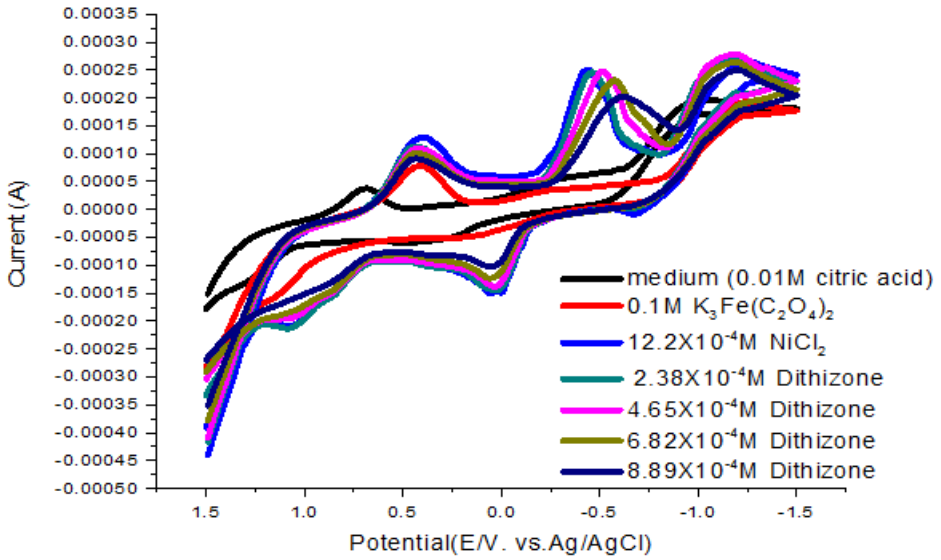

Figure-2. Cyclic voltamogram of $NiCl_2$ (0.1M) with dithizone ligand at 293.15K.

Many sharp redox peaks of nickel ion on adding potassium ferrioxalate using gold electrode at 0.5V as reduction waves as shown in Figure 2.

Effect of scan rates on cmplexation was studied and the redox mechanism was presented in Table 3 and Figure 3 indicating quasi reversible and diffusion mechanisms.

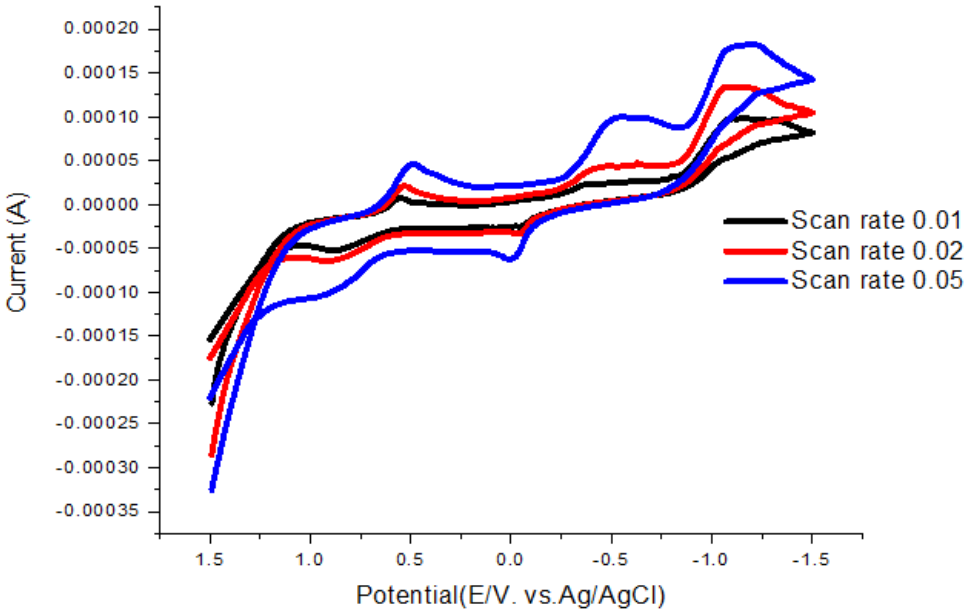

Figure-3. Scan rate of dithizone –$NiCl_2$ complex at 293.15K.

At 303.15 K, the oxidation peaks was observed at approximately -0.033V as shown in Figure 4 and the electrochemical kinetic parameters were determined and are listed in Table 4. By adding different concentrations of dithizone ligand from the range of $2.33X10^{-4}$ to $5.62X10^{-4}$ M we noted shift and increasing on the peak of redox reaction suggesting the formation of complexes.

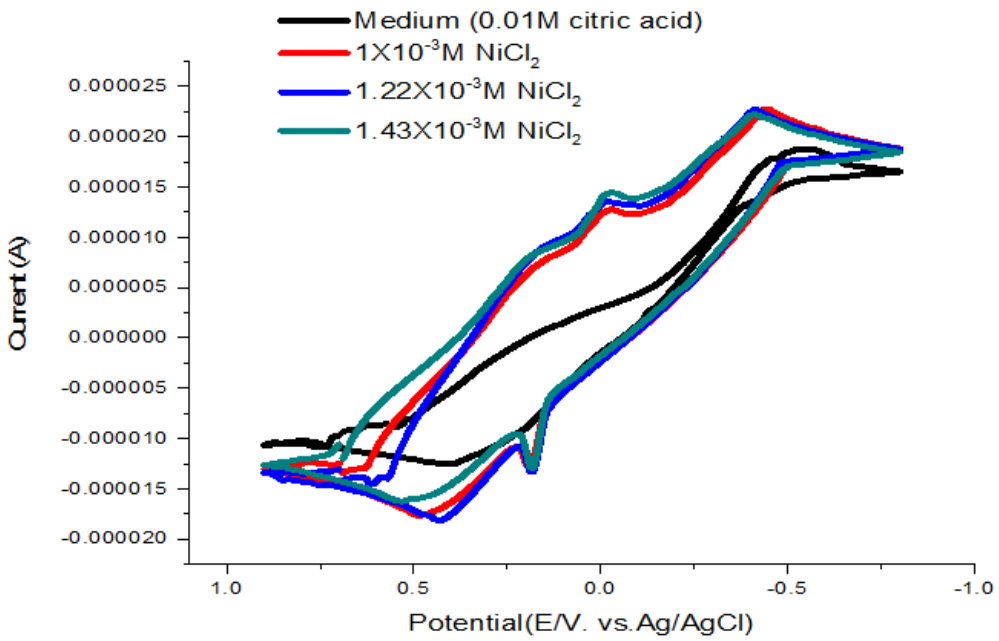

Figure-4. Cyclic voltamogram of $NiCl_2$ (0.1M) in citric acid media at303.15K.

The peak of complex decreased by increasing the concentration of dithizone ligand as shown in Figure 5 and the complex parameters are tabulated in Table 5.

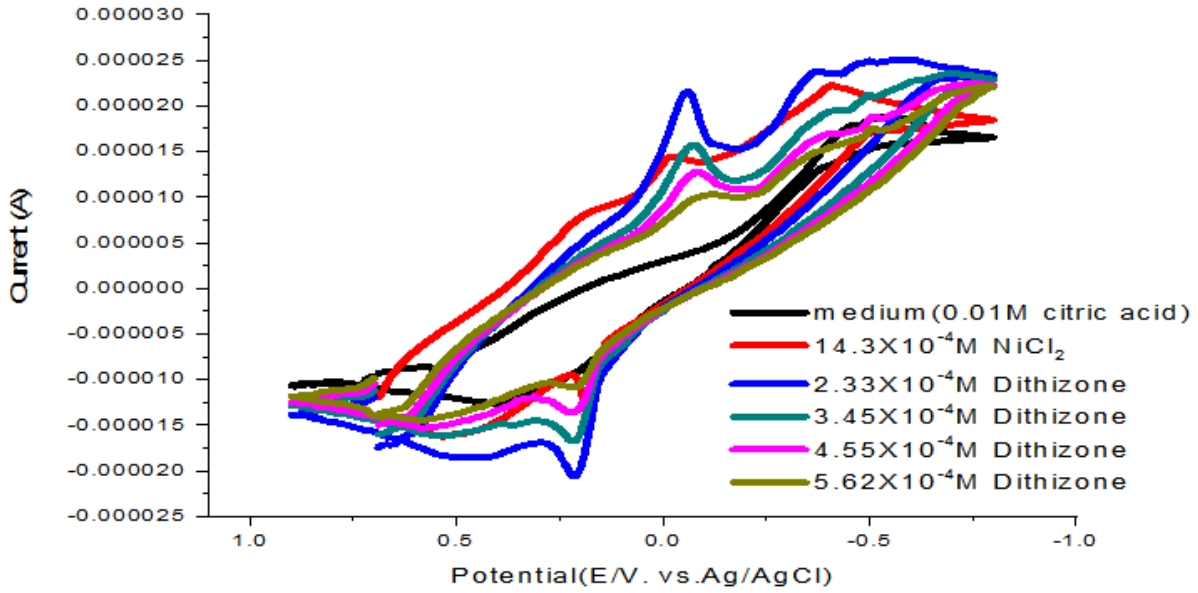

Figure-5. Cycic voltamogram of $NiCl_2$ (0.1M) with dithizone ligand at 303.15K.

Scan rate effect on complex formation was studied and the redox mechanism was presented in Table 6 and Figure 6 indicating quasi reversible and diffusion mechanisms.

Table-5. Electrochemical parameters of complex formation at 303.15 K.

[L] $x10^{-4}$	Ep,a (volt)	(-)Ep,c (volt)	ΔEp (volt)	ipa $x10^{-6}$ (Amp)	ipc $x10^{-6}$ (Amp)	ipa/ ipc	Da $x10^{-13}$	Dc $x10^{-13}$	(-)Epc/2	αna	ks $x10^{-4}$	Γc $x10^{-10}$ (mol/cm2)	(+) Qc $x10^{-6}$	Γa $x10^{-10}$ (mol/cm2)	(-)Qa 10^{-6}
2.33	0.2107	0.0587	0.2693	7.69	8.53	0.9018	3.2491	3.9955	0.0148	1.1047	4.91	5.882	4.4551	5.3044	4.0175
3.45	0.2117	0.0758	0.2875	6.01	5.66	1.0613	1.9834	1.7607	0.0249	0.9525	4.29	3.9047	2.9575	4.1443	3.1389
4.55	0.2119	0.0811	0.2931	3.78	3.45	1.0949	0.78549	0.65519	0.0384	1.1355	3.18	2.3819	1.8041	2.608	1.9754
5.62	0.2005	0.1184	0.3188	1.71	1.49	1.1513	0.16128	0.12168	0.0638	0.8887	1.98	1.0264	0.77746	1.1818	0.89508

Table-6. Scan rate kinetic parameters of complex at 303.15 K.

υ	M $x10^{-3}$	Ep,a (volt)	(-)Ep,c (volt)	ΔEp (volt)	(-)ipa $x10^{-6}$ (Amp)	ipc $x10^{-6}$ (Amp)	ipa/ ipc	Da $x10^{-15}$	Dc $x10^{-14}$	(-)Epc/2	αna	ks $x10^{-2}$	Γc $x10^{-10}$ (mol/cm2)	(+) Qc $x10^{-5}$	Γa $x10^{-10}$ (mol/cm2)	(-)Qa 10^{-6}
0.01	1.43	0.0939	0.2995	0.39	0.0894	0.701	0.1276	0.44	2.698	0.2744	1.94	0.057	4.8335	0.37	0.61656	0.467
0.02	1.43	0.1374	0.3399	0.48	1.28	4.16	0.3075	45.04	47.63	0.284	0.87	1.14	14.36	1.09	4.4161	3.34
0.05	1.43	0.20983	0.4196	0.63	0.0419	0.477	0.0878	0.02	0.25	0.4079	4.16	5.26	0.65846	0.05	0.057806	0.0438

Table-7. Electrochemical parameters of NiCl2 in acidic media at 313.15K.

M $x10^{-3}$	Ep,a (volt)	Ep,c (volt)	ΔEp (volt)	(-)ipa $x10^{-5}$ (Amp)	ipc $x10^{-5}$ (Amp)	ipa/ ipc	Da $x10^{-10}$	Dc $x10^{-10}$	Epc/2	αna	ks $x10^{-3}$	Γc $x10^{-9}$ (mol/cm2)	(+) Qc $x10^{-5}$	Γa $x10^{-9}$ (mol/cm2)	(-)Qa 10^{-5}
0.526	0.3109	0.0595	0.2514	6.00	7.13	0.8407	1.4553	2.06	0.0972	1.3298	7.32	5.0821	3.85	4.2723	3.24
0.769	0.2997	0.06	0.2396	5.81	7.38	0.7875	0.64076	1.03	0.1009	1.2273	4.01	5.2614	3.98	4.1432	3.14
1.00	0.2875	0.0509	0.2366	5.98	8.92	0.6703	0.40061	0.892	0.0979	1.0651	3.28	6.3537	4.81	4.2589	3.23
1.22	0.2776	0.0511	0.2265	6.02	8.56	0.7033	0.27328	0.552	0.0934	1.1833	2.26	6.0992	4.62	4.2897	3.25
1.43	0.2713	0.0499	0.2213	6.49	9.51	0.6819	0.23121	0.497	0.0923	1.1823	1.94	6.7778	5.13	4.6221	3.50

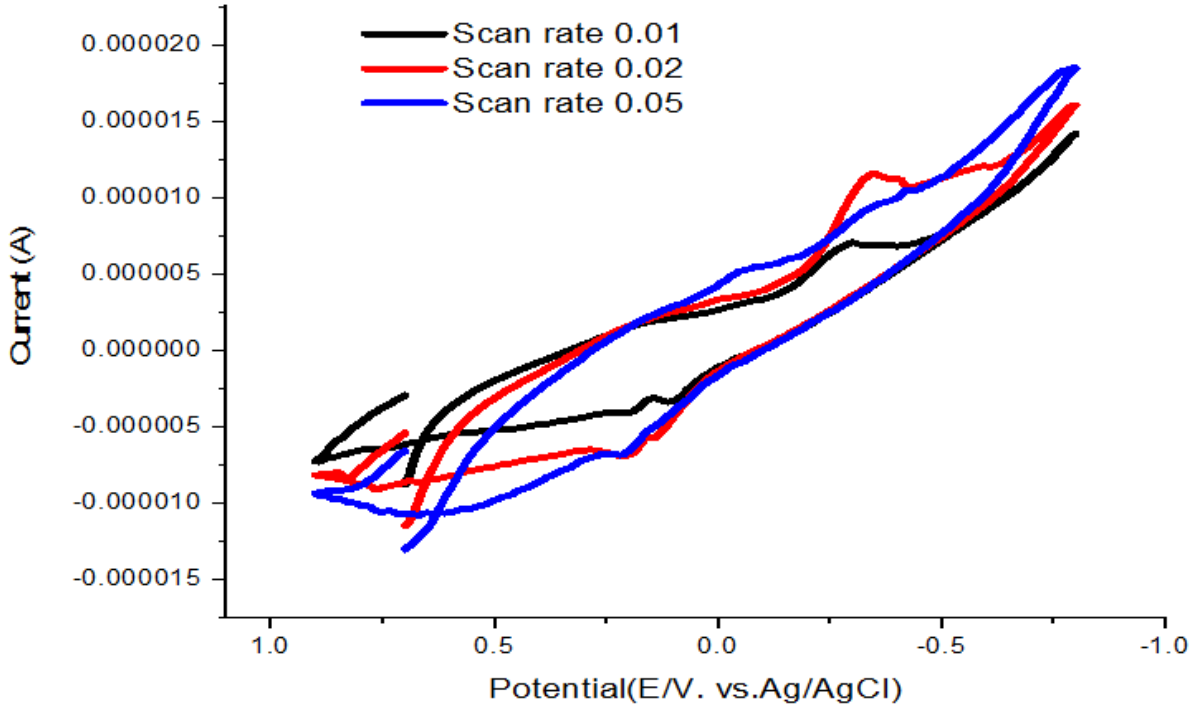

Figure-6. Scan rate of dithizone –$NiCl_2$ complex at 303.15K.

At 313.15K the oxidation peak at approximately 0.1V as shown in Figure 7 and the electrochemical kinetic parameters are presented in Table 7.

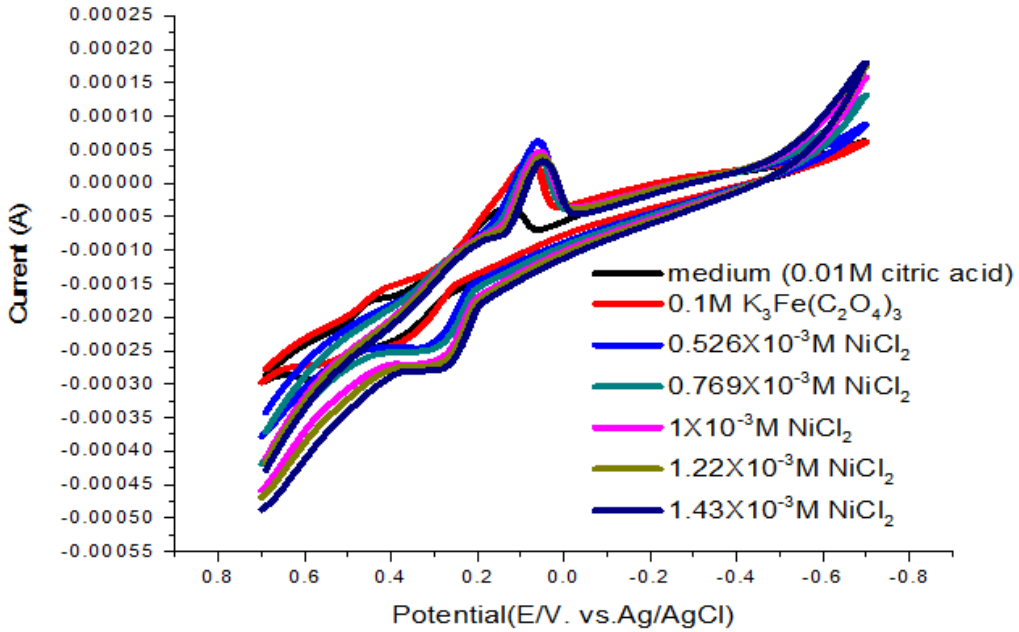

Figure-7. Cyclic voltamogram of $NiCl_2$ (0.1M) in citric acid media at313.15K.

When started adding different concentrations of dithizone ligand from the range of 1.37X10^{-4} to 7.69X10^{-4} M we observed shift in redox peak as shown in Figure 8 which explained the formation of complex. We listed the complex electrochemical kinetic parameters in Table 8.

Table-8. Electrochemical parameters of complex formation at 313.15K.

[L] x10^{-4}	Ep,a (volt)	Ep,c (volt)	ΔEp (volt)	(-)ipa x10^{-5} (Amp)	ipc x10^{-5} (Amp)	ipa/ ipc	Da x10^{-11}	Dc x10^{-12}	Epc/2	αna	ks x10^{-4}	Γc x10^{-9} (mol/cm2)	(+) Qc x10^{-6}	Γa x10^{-9} (mol/cm2)	(-)Qa 10^{-5}
1.37	0.3202	0.0363	0.2839	11.4	0.461	24.8603	7.2026	0.117	0.04862	4.0533	5.56	0.32816	2.49	8.158	6.18
2.70	0.3108	0.0498	0.2609	7.38	0.281	26.2622	2.9885	0.0433	0.0542	11.2321	3.69	0.20009	1.52	5.2549	3.98
4.00	0.3107	0.0317	0.279	8.11	0.684	11.8532	3.6118	0.257	0.04967	2.7938	6.26	0.48738	3.69	5.777	4.38
5.26	0.3106	0.01	0.3007	7.34	0.772	9.5101	2.9604	0.327	0.0387	1.7459	8.33	0.54996	4.17	5.2302	3.96
6.49	0.2999	-0.0035	0.3035	6.45	1.37	4.6967	2.2829	1.03	0.0219	1.9673	16.6	0.97789	7.41	4.5929	3.48
7.69	0.2987	-0.0106	0.3093	6.58	1.72E	3.8326	2.3788	1.62	0.0229	1.4934	20.1	1.2233	9.27	4.6883	3.55

Table-9. Scan rate kinetic parameters of complex at 313.15K.

υ	M x10^{-3}	Ep,a (volt)	Ep,c (volt)	ΔEp (volt)	(-)ipa x10^{-5} (Amp)	ipc x10^{-5} (Amp)	ipa/ ipc	Da x10^{-11}	Dc x10^{-11}	Epc/2	αna	ks x10^{-4}	Γc x10^{-9} (mol/cm2)	(+) Qc x10^{-5}	Γa x10^{-9} (mol/cm2)	(-)Qa 10^{-5}
0.05	1.43	0.2894	0.0409	0.2485	4.57	3.09	1.4764	2.2929	1.0519	0.08	1.2811	10.9	4.4089	3.34	6.5094	4.93
0.02	1.43	0.2702	0.0697	0.2005	2.78	0.512	5.4286	2.1193	0.071916	0.0789	5.4498	1.53	1.8228	1.38	9.8952	7.49
0.01	1.43	0.26	0.0873	0.1728	1.65	0.132	12.4656	1.4967	0.00963	0.0918	11.2446	0.339	0.94339	0.715	11.759	8.91

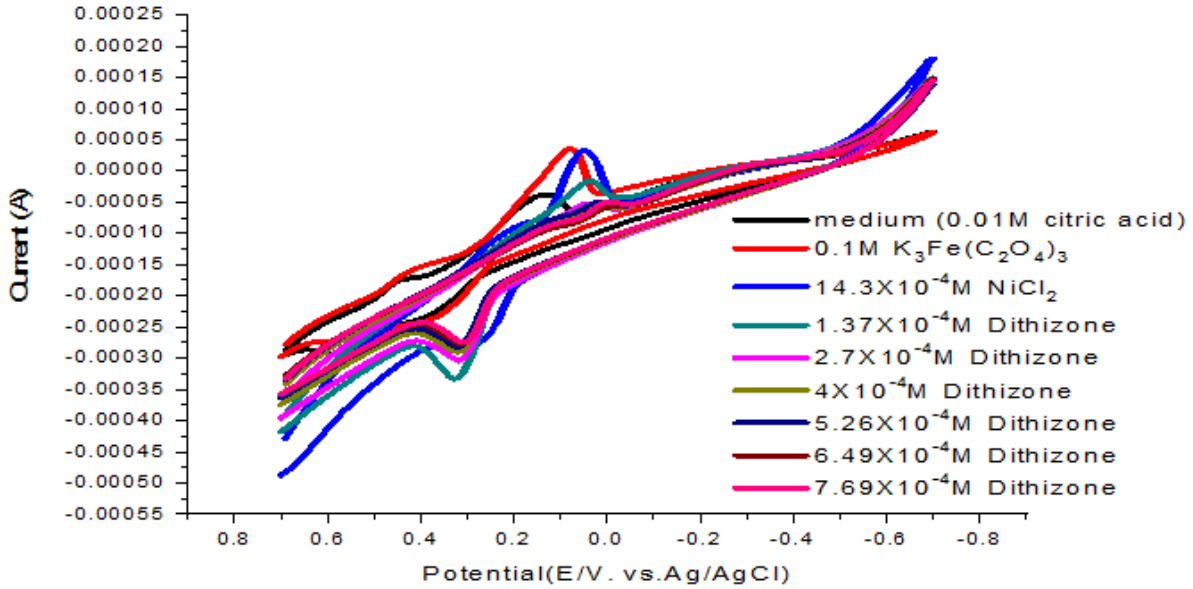

Figure-8. Cyclic voltamogram of $NiCl_2$ (0.1M) with dithizone ligand at 313.15K.

Complexation scan rate effect was studied and the redox mechanism was presented in Table 9 and Figure 9 indicating quasi reversible and diffusion mechanism.

All the cyclic voltammetry date show decrease in their values by decrease of the scan rate especially the value of k_s the rate constant for electron transfer which indicate that the reaction is diffusion controlled.

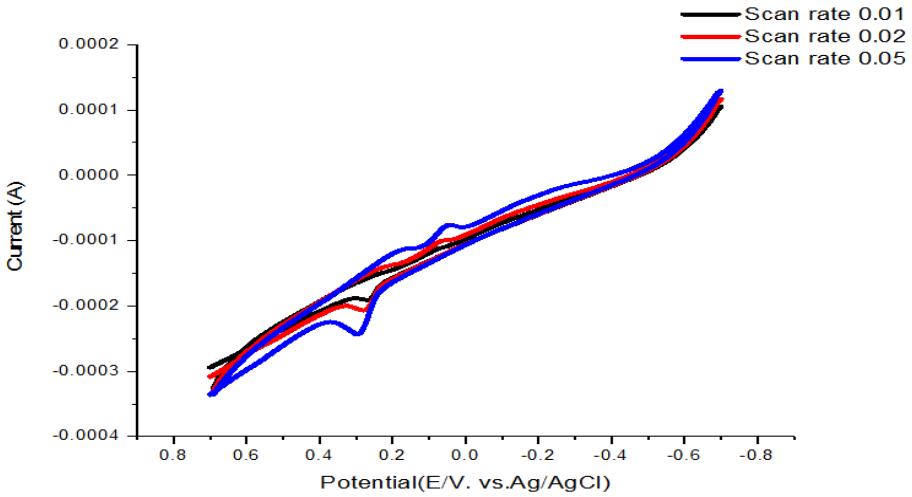

Figure-9. Scan rate of dithizone –$NiCl_2$ complex at 313.15K.

3.3. Electrochemical Behavior and Thermodynamic Parameters for Dithizone-Ni Complex

In this work, we are studying the electrochemical behavior of the complexation between dithizone ligand and $NiCl_2$ at different temperature (293.15, 303.15, and 313.15 K).

A stability constant is a measure of the strength of the interaction between the reagents that come together to form the complex. The stability constants (β_{MX}) for nickel chloride complexes are calculated by applying Equation 10:

$$\Delta E^\circ = E^\circ_C - E^\circ_M = 2{:}303\,(RT/nF) * (\log \beta_{MX} + j\log C_x) \qquad (10)$$

where E°_M is the formal peak potential of metal in the absence of ligand, E°_C is the formal peak potential of metal complex after each addition of dithizone ligand, R is a gas constant (8.314 J $mol^{-1}K^{-1}$), T is the absolute temperature, j is the coordination number of the stoichiometric complex and C_x is the concentration of ligand in the solution.

The formal potential E° can be found as the midway between the two cyclic voltammetry peaks comprising the voltammogram by Equation 11:

$$E^\circ = (E_{pa} + E_{pc})/2 \qquad (11)$$

where both E_{pa} and E_{pc} are anodic peak potential and cathodic peak potential, respectively.

The Gibbs free energy of interaction for nickel chloride with dithizone were calculated from stability constant (β_{MX}) using Equation 12 [14, 20-28]:

$\Delta G = -2{:}303\ RT \log \beta_{MX}$ (12)

All equilibrium constant vary with temperature, so the enthalpy (ΔH) of interaction for $NiCl_2$ with dithizone ligand was calculated by using Van't Hoff Equation 13:

$$\log (\beta_{MX} \text{ at } (T_2)/ \beta_{MX} \text{ at } (T_1)) = (\Delta H/2.303)((T_2T_1)/T_2\text{-}T_1) \quad (13)$$

where β_{MX} is the stability constant at different temperatures.

The entropy (ΔS) at different temperatures are calculated by using Equation 14:

$\Delta S = (\Delta H\text{-}\Delta G)/T$ (14)

The thermodynamic parameters of nickel Chloride with dithizone at different temperatures (293.15, 303.15, and 313.15 K) are listed in Tables 10-12 respectively.

Table-10. Cyclic voltammetry data of dithizone and $NiCl_2$ complex at 239.15 K.

[L] X10^{-4}	- E°$_M$	E°$_C$	ΔE mv	j	log βj	-ΔG (KJ/mol)	ΔH (KJ/mol)	ΔS (KJ/mol)
2.38	0.0024	0.0207	0.0231	0.2	1.5184	8.5231	74.9933	0.2848
4.65	0.0024	0.0242	0.0266	0.4	2.2471	12.6130	187.3402	0.6820
6.82	0.0024	0.0435	0.0459	0.6	3.47884	19.5266	191.1450	0.7186
8.89	0.0024	0.0436	0.0461	0.8	4.02202	22.5755	249.856	0.9293

Table-11. Cyclic voltammetry data of dithizone and $NiCl_2$ complex at 303.15 K.

[L] X10^{-4}	E°$_M$	E°$_C$	ΔE mv	J	log βj	-ΔG (KJ/mol)	ΔH (KJ/mol)	ΔS (KJ/mol)
2.33	0.1817	0.2107	0.0289	0.1667	1.5693	9.1092	74.9933	0.2694
3.45	0.1817	0.2117	0.03	0.25	1.86483	10.8243	187.3402	0.2371
4.55	0.1817	0.2119	0.0303	0.3333	2.1212	12.3127	191.1450	0.2176
5.62	0.1817	0.2005	0.0188	0.4167	1.9796	11.4909	249.856	0.2276

Table-12. Cyclic voltammetry data of dithizone and $NiCl_2$ complex at 313.15 K.

[L] X10^{-4}	(Ep,a)M	(Ep,a)C	ΔE mv	J	log βj	-ΔG (KJ/mol)	ΔH (KJ/mol)	ΔS (KJ/mol)
1.18	0.2713	0.3202	0.0489	0.0833	1.9022	11.4059	74.9933	0.2275
2.33	0.2713	0.3108	0.0395	0.1667	1.8766	11.2522	187.3402	0.4246
3.45	0.2713	0.3107	0.0394	0.2500	2.1362	12.8085	191.1450	0.6702
4.55	0.2713	0.3106	0.0393	0.3333	2.3831	14.2894	249.8560	0.7479
5.62	0.2713	0.2999	0.0287	0.4167	2.2784	13.6615	260..8458	0.9755
6.67	0.2713	0.2987	0.0275	0.5	2.4725	14.8253	282.8302	1.1032

The different thermodynamic data given in Table 10.Table 11, Table 12, are calculated from the cyclic voltammetry measured voltammograms and following equations,Equation 10.Equation 11 and Equation 12.

The Gibbs free energies for the complex interaction between $NiCl_2$ and dithizone are slightly increased by the increase of temperature indicating the increase of the kinetic energy of the interacting system. The entropies of solvation of the complex formed gave not sufficient indication because of their small values.

3.4. Molecular Docking

Molecular docking is a key tool in computer drug design. The focus of molecular docking is to simulate the molecular recognition process. Molecular docking aims to achieve an optimized conformation for both the protein and drug with relative orientation between them such that the free energy of the overall system is minimized. In this context, the docked ligand was analysis with the human liver cancer 3cmf Hormone as shown in Figure 10.

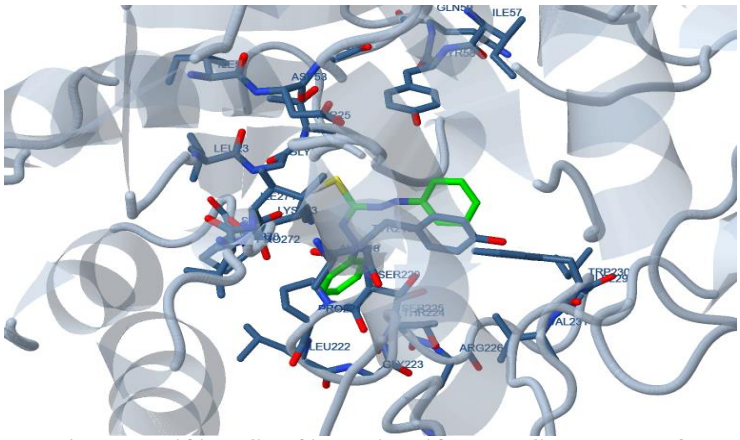

Figure-10. Dithizone ligand interaction with receptor liver cancer 3cmf.
Source: The source of Figure 10 is the theoretical calculations.

The study simulates the actual docking process in which the ligand-protein pairwise interaction energies are calculated. The docking results are described in Table 13. From the analysis of the values, it is evident that the binding energy of the mutated ligand is less than that of unmutated ligand. Binding energies are most widely used mode of measuring binding affinity of a ligand. Thus, decrease in binding energy due to mutation will increase the binding affinity to the dithizone ligand.

Table-13. Energy values obtained in docking calculations of dithizone ligand with receptor liver cancer 3cmf.

Rank	Est. Free Energy of Binding (kcal/mol)	Est. Inhibition Constant, Ki(uM)	vdW + Hbond + desolv Energy (kcal/mol)	Electrostatic Energy (kcal/mol)	Total Intermolec. Energy (kcal/mol)
1.	-7.44	3.54	-8.42	-0.06	-8.48
2.	-7.11	6.13	-8.21	-0.02	-8.22
3.	-5.71	65.67	-6.84	+0.02	-6.82
4.	-5.48	96.93	-6.57	+0.01	-6.57
5.	-5.44	102.55	-7.30	-0.03	-7.33

According to our results, HB plot curve indicate that, ligand binds to the protein with hydrogen bond. Interactions of ligand with 3cmf are shown in Figure 11. The calculated efficiency is favorable, Ki values estimated by AutoDock were compared with experimental Ki values, when available, and the Gibbs free energy is negative. Also, based on this data, we can propose that interaction between the 3cmf receptors and the ligand is possible.

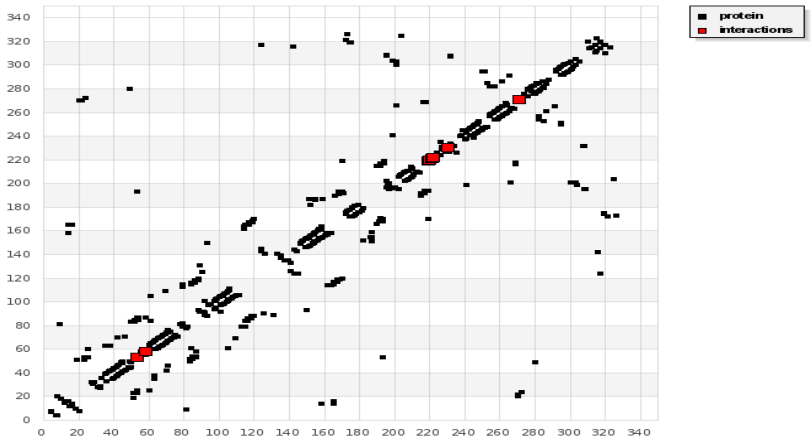

Figur-11. 2D plot curve of docking with ligand (HL) are shown in Figure 12. This interaction could activate apoptosis in cancer cells energy of interactions with ligand.

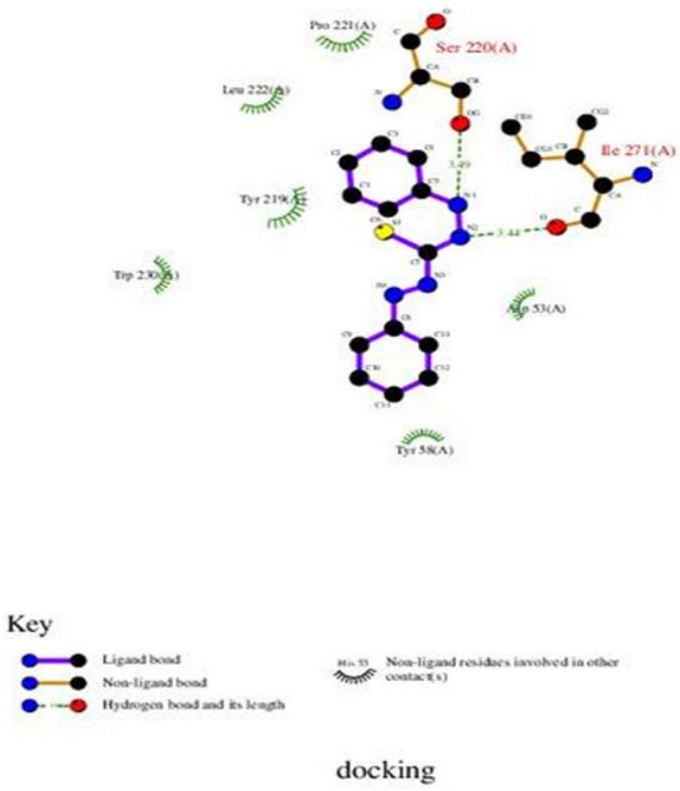

Figure-12. 2D plot of interaction between the ligand and receptor liver cancer 3cmf.

4. Conclusion

The electrochemical behavior reduction or and oxidation [29, 30] of $NiCl_2$ was studied at different temperatures (293.15, 303.15, and 313.15K) in the presence of potassium ferrioxalate as mediators in 0.1 M citric acid since normally nickel ions gave no waves in acidic media. This method is simple to discuss the electrochemical behavior of Ni(II) ions. The cyclic voltammetry parameters were obtained for the electro redox reaction of nickel chloride in absence and presence of dithizone (diphenylthiocarbazone}. The measured $NiCl_2$ cyclic voltammetry was developed at different scan rates, which prove that electron transfer reaction was diffusion controlled in absence and presence of dithizone.

References

[1] C. G. Zoski, *Handbook of electrochemistry*. Amsterdam, The Netherlands: Elsevier, Amsterdam, 2006.

[2] S. Tanimoto and A. Ichimura, "Discrimination of inner-and outer-sphere electrode reactions by cyclic voltammetry experiments," *Journal of Chemical Education*, vol. 90, pp. 778-781, 2013.Available at: https://doi.org/10.1021/ed200604m.

[3] S. J. Hendel and E. R. Young, "Introduction to electrochemistry and the use of electrochemistry to synthesize and evaluate catalysts for water oxidation and reduction," *Journal of Chemical Education*, vol. 93, pp. 1951-1956, 2016.Available at: https://doi.org/10.1021/acs.jchemed.6b00230.

[4] K. Schmidt-Rohr, "How batteries store and release energy: Explaining basic electrochemistry," *Journal of Chemical Education*, vol. 95, pp. 1801-1810, 2018.Available at: https://doi.org/10.1021/acs.jchemed.8b00479.

[5] T. Ayodele, O. Dularu, A. A. Peter, and Z. M. Johannes, "Impact of molybdenum compounds as anticancer agents," *Hindawi, Bioinorganic Chemistry and Applications*, pp. 1-10, 2019.Available at: 10.11555/2019/6416198.

[6] D. Polo-Cero´n, "Cu(II) and Ni(II) complexes with new tridentate NNS thiosemicarbazones: Synthesis, Characterisation, DNA Interaction, and Antibacterial Activity," *Hindawi .Bioinorganic Chemistry and Applications*, vol. 2019, pp. 1-15, 2019.Available at: 10.1155/2019/3520837.

[7] J. T. Groves, "The bioinorganic chemistry of iron in oxygenases and supramolecular assemblies," *Proceedings of the National Academy of Sciences*, vol. 100, pp. 3569-3574, 2003.

[8] I. Bertini and A. Rosato, "Bioinorganic chemistry in the postgenomic era," *Proceedings of the National Academy of Sciences*, vol. 100, pp. 3601-3604, 2003.Available at: 10.1073/pnas.0736657100.

[9] E. A. Gomaa and R. M. Abu-Qarn, "Ionic association and thermodynamic parameters for solvation of vanadyl sulfate in ethanol-water mixtures at different temperatures," *Journal of Molecular Liquids*, vol. 232, pp. 319-324, 2017.

[10] E. A. Gomaa and M. A. Tahoon, "Ion association and solvation behavior of copper sulfate in binary aqueous–methanol mixtures at different temperatures," *Journal of Molecular Liquids*, vol. 214, pp. 19-23, 2016.

[11] E. Gomaa, R. Zaky, and A. Shokr, "Estimated the physical parameters of lanthanum chloride in water-N, N-dimethyl formamide mixtures using different techniques," *Journal of Molecular Liquids*, vol. 242, pp. 913-918, 2017.

[12] E. Gomaa, R. Zaky, and A. Shokr, "Effect of calcon carboxylic acid on association process of vanadyl sulfate in water-N, N-dimethyl formamide mixed solvents," *Chemical Data Collections*, vol. 11, pp. 67-76, 2017.
[13] C. H. Bamford, C. F. H. Tipper, and R. G. Compton, *Electrode kinetics: Principles and methology* vol. 26. New York: Elsevier, 1986.
[14] D. A. C. Brownson and C. E. Banks, *The handbook of graphene electrochemistry*. New York: Springer, 2014.
[15] Y. Wang, R. M. Hernandez, D. J. Bartlett, J. M. Bingham, T. R. Kline, A. Sen, and T. E. Mallouk, "Bipolar electrochemical mechanism for the propulsion of catalytic nanomotors in hydrogen peroxide solutions," *Langmuir*, vol. 22, pp. 10451-10456, 2006.
[16] A. E. El-Askalany and E.-H. Abdel-Monem, "Stability Constants of Zn (II), Pb (II), Cd (II) and Cu (II) Complexes with Hymatoxylin," *Chemical and pharmaceutical bulletin*, vol. 43, pp. 1791-1792, 1995.
[17] E. A. Gomaa, A. Negm, and M. A. Tahoon, "Conductometric and volumetric study of copper sulphate in aqueous ethanol solutions at different temperatures," *Journal of Taibah University for Science*, vol. 11, pp. 741-748, 2017.
[18] S. El-Shereafy, E. Gomaa, A. Yousif, and A. Abou Elyazed, "Electrochemical and thermodynamic estimations of the interaction parameters for bulk and nano-silver nitrate (NSN) with cefdinir drug using a glassy carbon electrode," *Iranian Journal of Materials Science and Engineering*, vol. 14, pp. 48-57, 2017.
[19] J. I. Kim, A. Cecal, H. J. Born, and E. A. Gomaa, "Preferential solvation of single ion: acritical study of the Ph4AsPh4B Assumption for single ion thermodynamics in mixed aqueous-acetonitrile and Aqueous-N,N-dimethyl Formamide Solvents," *Z. Phys. Chem., Neue Folge*, vol. 110 pp. 209-218, 1978.
[20] J. Kim and E. Gomaa, "Preferential solvation of single Ions: The PH4ASPH4B assumption for single Ion thermodynamics in mixed dimethylsulfoxide-water solvents," *Bulletin des Sociétés Chimiques Belges*, vol. 90, pp. 391-407, 1981.
[21] M. Ghandour, R. Abo-Doma, and E. Gomaa, "The electroreduction (polarographically) of uranyl ion in nitric acid and nitric acid-methanol mixture media," *Electrochimica Acta*, vol. 27, pp. 159-163, 1982.
[22] E. Gomaa, "Thermodynamic studies of the solvation of Ph4AsPh4B in mixed solvents (MeOH—DMF)," *Thermochimica Acta*, vol. 80, pp. 355-359, 1984.
[23] A. K. Abd-Elkader, E. A. Gomaa, and A. H. El-Askalany, "Polarographic electro-reduction of nitroprusside ion," *Acta Chimica Hung*, vol. 118, pp. 197-212, 1985.
[24] M. Abd El-Hady, E. A. Gomaa, and A. G. Al-Harazie, "Cyclic voltammetry of bulk and nano CdCl2 with ceftazidime drug and some DFT calculations," *Journal of Molecular Liquids*, vol. 276, pp. 970-985, 2019.
[25] R. S. Nicholson, "Theory and application of cyclic voltammetry for measurement of electrode reaction kinetics," *Analytical Chemistry*, vol. 37, pp. 1351-1355, 1965.
[26] G. A. Mabbott, "An introduction to cyclic voltammetry," *Journal of Chemical Education*, vol. 60, pp. 697-702, 1983.
[27] E. A. Gomaa, M. H. Mahmoud, M. G. Mousa, and E. M. El-Dahshan, "Cyclic voltammetry for the interaction between bismuth nitrate and methyl red in potassium nitrate solutions," *Chemical Methodologies*, vol. 3, pp. 1-11, 2018.
[28] M. Abd El-Hady, E. Gomaa, R. Zaky, and A. Gomaa, "Synthesis, characterization, computational simulation, cyclic voltammetry and biological studies on Cu (II), Hg (II) and Mn (II) complexes of 3-(3, 5-dimethylpyrazol-1-yl)-3-oxopropionitrile," *Journal of Molecular Liquids*, p. 112794, 2020.Available at: 10.1016/j.molliq.2020.112791.
[29] A. H. A. Shah, A. Inayat, and S. Bilal, "Enhanced eectrocatalytic behavior of poly(anline-Co-2-hydroxyanline) coated electrodes, for hydrogen peroxide electrooxidation," *Catalysis*, vol. 631, pp. 1-16, 2019.
[30] Y. Guo, D. He, A. Xie, W. Qu, Y. Tang, L. Zhou, and R. Zhu, "The electrochemical oxidation of hydroquinone and catechol through a novel poly-gemineral dicationic liquid (PGDIL)-TiO2 composite film electrode," *Polymer*, vol. 11, pp. 1-17, 2019.